

Nancy Rehak¹, D. Megenhardt, C. K. Mueller
National Center for Atmospheric Research²

1 INTRODUCTION

Tsonis and Austin (1981) first investigated the use of trends in echo size and intensity to improve forecasts out to 30 minutes. Trending was further tested by Wilson et al. (1998) using the Thunderstorm Identification, Tracking, Analysis and Nowcasting system (Dixon et al., 1993) for forecasts ranging between 6 and 36 minutes. In both cases, little if any improvement was found. Wilson et al. (1998) concluded that “essential physical processes that dictate the change in rainfall with time are not necessarily observable in the past history of a particular echo development.” However, in an analysis of 0-2 hour forecasts, Boldi et al. (2002) and Wolfson et al. (2004) suggest that trending provides benefit. The difference in these studies is one of scale. In the earlier studies, individual cells were tracked and trended. In the Boldi work, the area change of the region around an individual grid point was evaluated. Instead of evaluating whether an individual cell was growing or dissipating, all the cells within a region were examined.

The National Convective Weather Forecast – 2 (NCWF-2) product³ provides short-range (1- and 2-hour) probabilistic nowcasts of convection based on radar, lightning and RUC data. The NCWF-2 software trends large-scale growth and dissipation. Trends are calculated in Lagrangian space, based on motion vectors at forecast time, using a weighted linear fit of a mean value within a given-radius circle over a given

¹ Corresponding author address: Nancy Rehak, NCAR, P.O. Box 3000, Boulder, CO 80307; e-mail: rehak@ucar.edu.

² The National Center for Atmospheric Research is partially funded by the National Science Foundation. This research is partially sponsored by the National Science Foundation through an Interagency Agreement in response to requirements and funding by the Federal Aviation Administration’s Aviation Weather Research Program.

³ NCWF development is sponsored by the Federal Aviation Administration’s (FAA) Aviation Weather Research (AWR) program as part of the Convective Weather Product Development Team. The Convective Weather Product Development Team consists of MIT Lincoln Laboratories, National Severe Storms Laboratory (NSSL), National Weather Service’s Aviation Weather Center (AWC) and NCAR.

period. This paper reviews the trending methodology used in NCWF-2 and shows results of applying large-scale dissipation trending to the 1- and 2-hour forecasts.

2 TRENDING METHODOLOGY

Trending in the NCWF-2 is calculated in Lagrangian space. The idea is to follow each grid point back in time to see how the area around the point is changing. Figure 1 demonstrates how we are calculating the trend for a single grid square

In Figure 1 we have chosen a grid square that falls within a line. In this simplified example, we will be calculating the trend based on data at the current time, at 30 minutes ago and at 60 minutes ago. The data in this example is considered to be unit-less since the units of the data don’t affect the trending algorithm. To determine where the current grid square was located in the past grids, we use the current motion vectors calculated in another part of the NCWF-2 system.

Once we have the grid point’s location at each time period, we calculate a specified statistic for the data values within a given-radius circle around the location in each grid. In the NCWF-2 system we are calculating the mean within a 30-km radius of influence. The software we are using also allows us to use a maximum or a percent coverage statistic.

When we have all of the statistics (means) for the given grid point, we are ready to calculate the trend using equation (1). In this equation, x is the time difference between the data time and the current time; y is the mean value of the data within the radius of influence; and w is the weight given to the time offset.

$$T = \frac{(\sum w * \sum xyw) - (\sum xw * \sum yw)}{(\sum w * \sum x^2w) - (\sum xw)^2} \quad (1)$$

If we assume in this example that we are giving a weight of 1.0 to the current data, a weight of 0.75 to the data that is 30 minutes old and a weight of 0.5 to the data that is 60 minutes old, we get a trend of 11.76 units/hr for the current grid point.

Growth and dissipation trends in the NCWF-2 system are calculated based on a field that represents the area coverage of VIL greater than 3.5 kg/m². So our resulting trend value is a percent change in area coverage per hour. The weight for each time period is specified in Table 1.

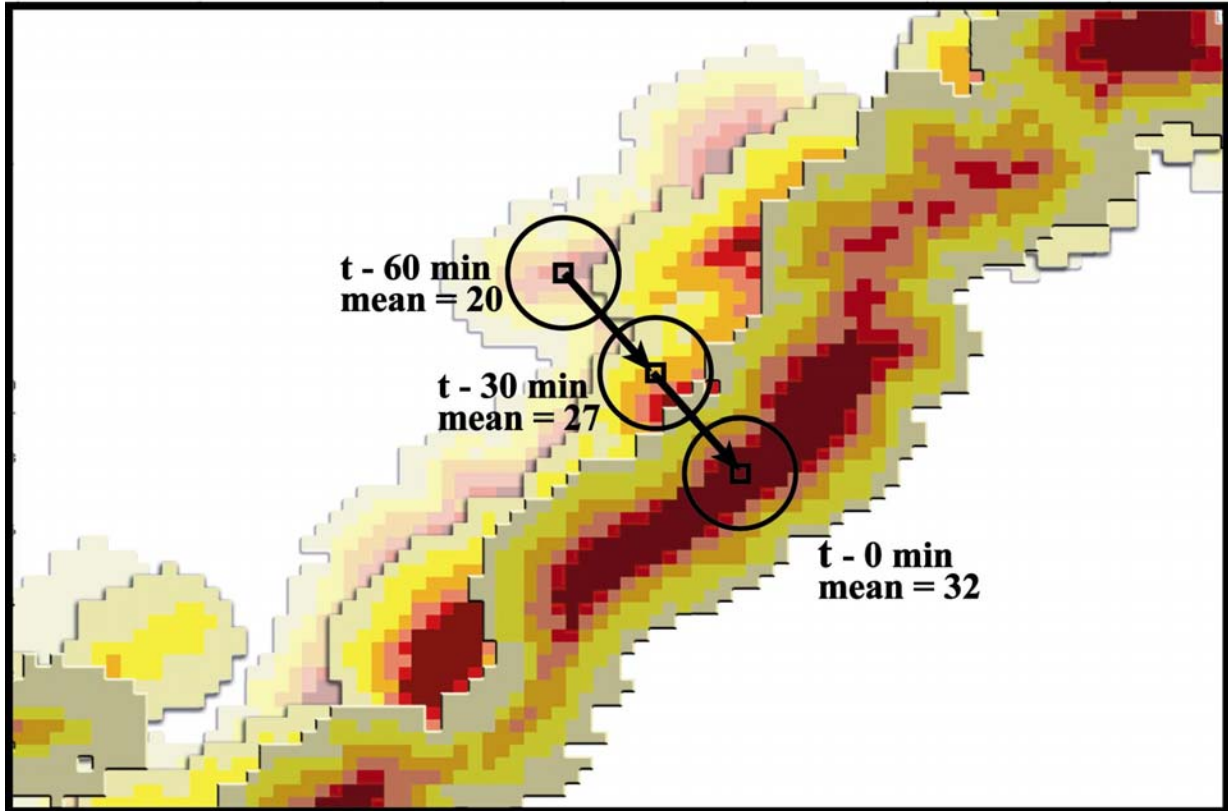


Figure 1 Illustration of the trending algorithm used in NCWF-2. The circles show the radius of influence around each location of the current grid point in time. In this example, the mean data value within the radius of influence at the current time is 32, the mean data value at the grid point's location 30 minutes ago is 27 and the mean data value 60 minutes ago is 20.

Time Offset in Minutes	Weight
0	1.0
5	1.0
10	1.0
15	1.0
20	0.5
25	0.4
30	0.3

Table 1. Time weighting in the NCWF-2 system.

The 1- and 2-hour forecasts produced by the NCWF-2 system use the calculated trends to reduce the probabilities in the forecasts only in areas of dissipation. The growth trend isn't used in either forecast because

growth tends to happen very rapidly, on the order of 10 to 20 minutes, so the storm would be at its maximum before the growth could be detected in our system.

3 EXAMPLE FORECASTS

Example forecasts of a line of decaying cells from June 18, 2004 are shown in Figures 2 and 3. Figure 2a shows the CIWS VIL data color-coded to represent VIP levels 1-6 at 0100 and 0140Z, respectively. Figure 2b shows regions where storms are dissipating (the blue shading) based on the calculation of trends discussed in the previous section. Both periods, show a fair amount of dissipation along the line.

Figures 2c and 2e are the 1- and 2-hour probability forecasts that are not trended. The methodology for determining probabilities is discussed in Megenhardt et al. (2004). The probability values are based on the radar-echo coverage within the vicinity of a point in Lagrangian space. The distance (vicinity) from the point varies depending on the forecast length.

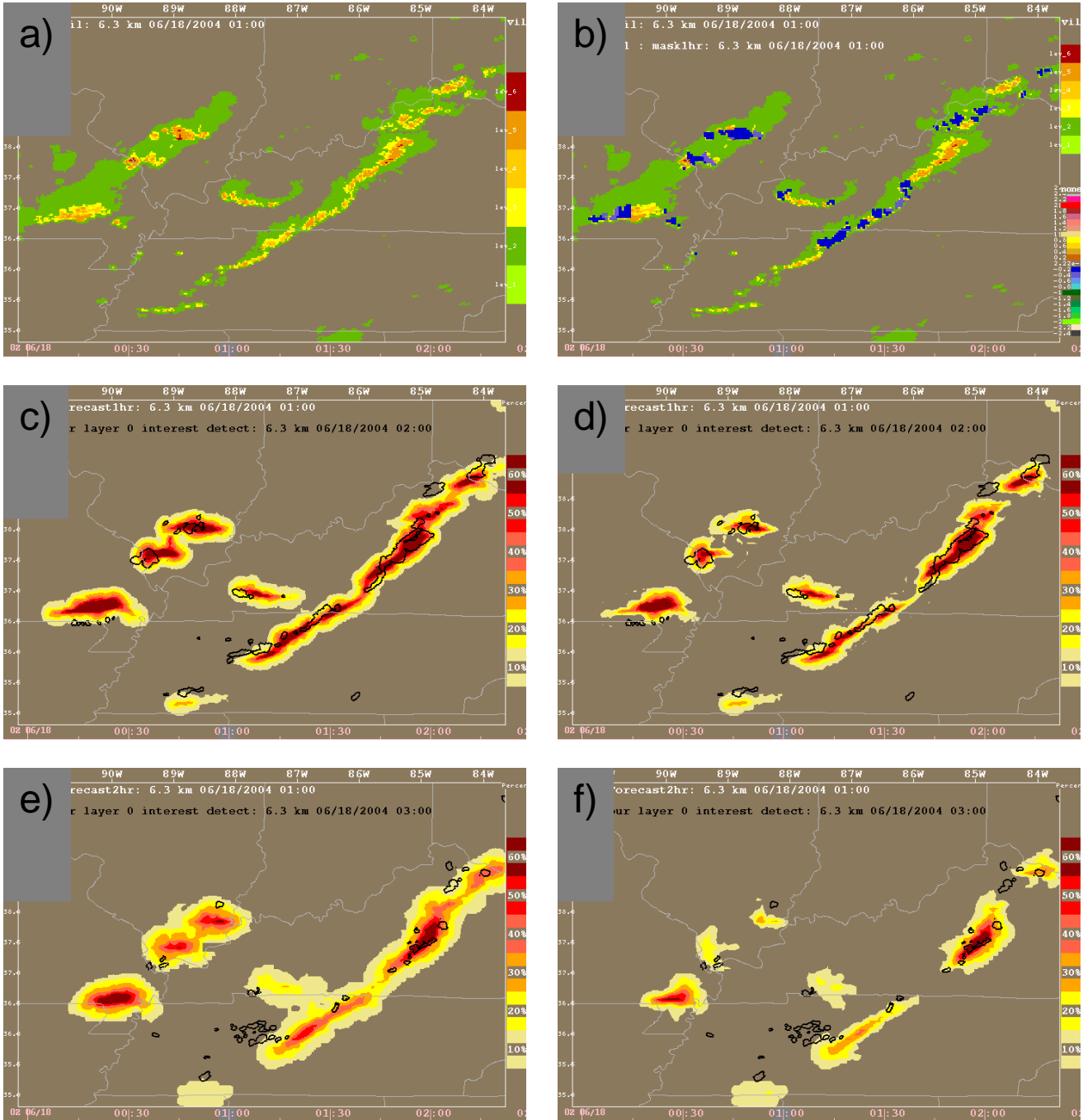


Figure 2 Shows example data and forecasts issued at 01Z on June 18, 2004. Figure 2a is the CIWS VIL data color-coded to represent VIP levels 1-6. Figure 2b shows regions of trended decay (blue) overlaid on the VIL data. Figures 2c and 2d show 1-hour probability forecasts without and with trending respectively. The color-table to the right of the image maps colors to the probability levels. Figures 2e and 2f show 2-hour probability forecasts with and without trending respectively. In Figures 2c, 2d, 2e, and 2f, forecast performance is illustrated by the black contours that indicate regions of level 3 or greater (VIL of 3.5) at the valid-time (verification observation).

Currently, the distance is set to 30 km for 1-hour forecasts and 50 km for 2-hour forecasts. This results in the 2-hour forecast having less detail and low-probability levels covering a larger region than the 1-hour forecasts. Forecast performance is illustrated by the

black contours that indicate regions of level 3 or greater (VIL of 3.5) at the valid-time (verification observation). As indicated by the figures, there is a strong tendency for over-forecasting in both the 1- and 2-hour periods.

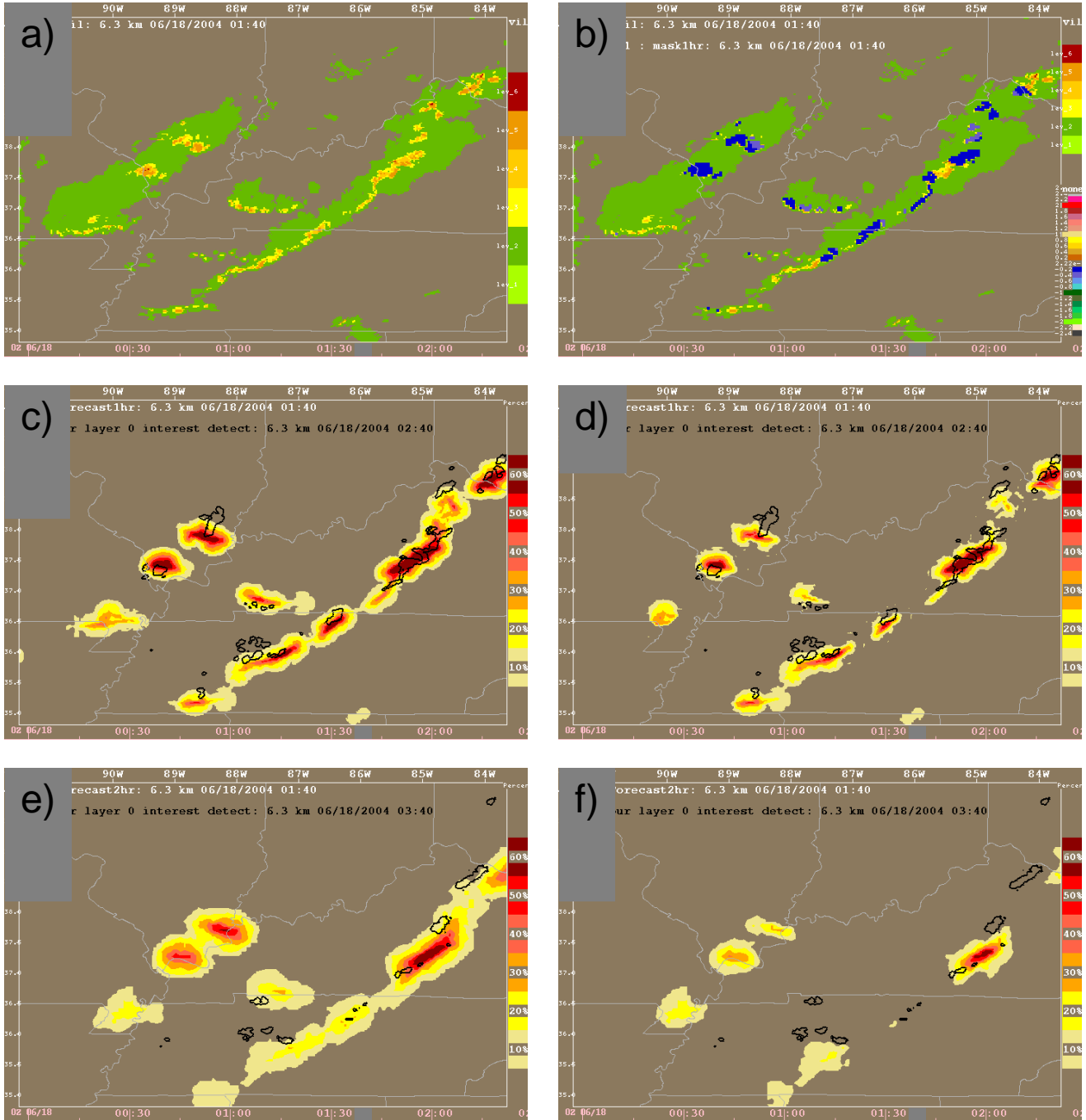


Figure 3 Same as Figure 2 except the data and forecasts were issued at 0140Z on June 18, 2004.

Figures 2d and 2f are the 1- and 2-hour forecasts with trended probabilities. The effect of trending is apparent because the forecast area decreases (compare Figure 2c with Figure 2d, and Figure 2e with Figure 2f). Also, gaps in the line become more apparent. This is especially true in the 2-hour forecasts (Figures 2e and

2f) along the Kentucky/Tennessee border. Visually, the regions of dissipation appear to be well represented in the trended probability forecasts and the trended forecasts appear to better represent the observations at this time.

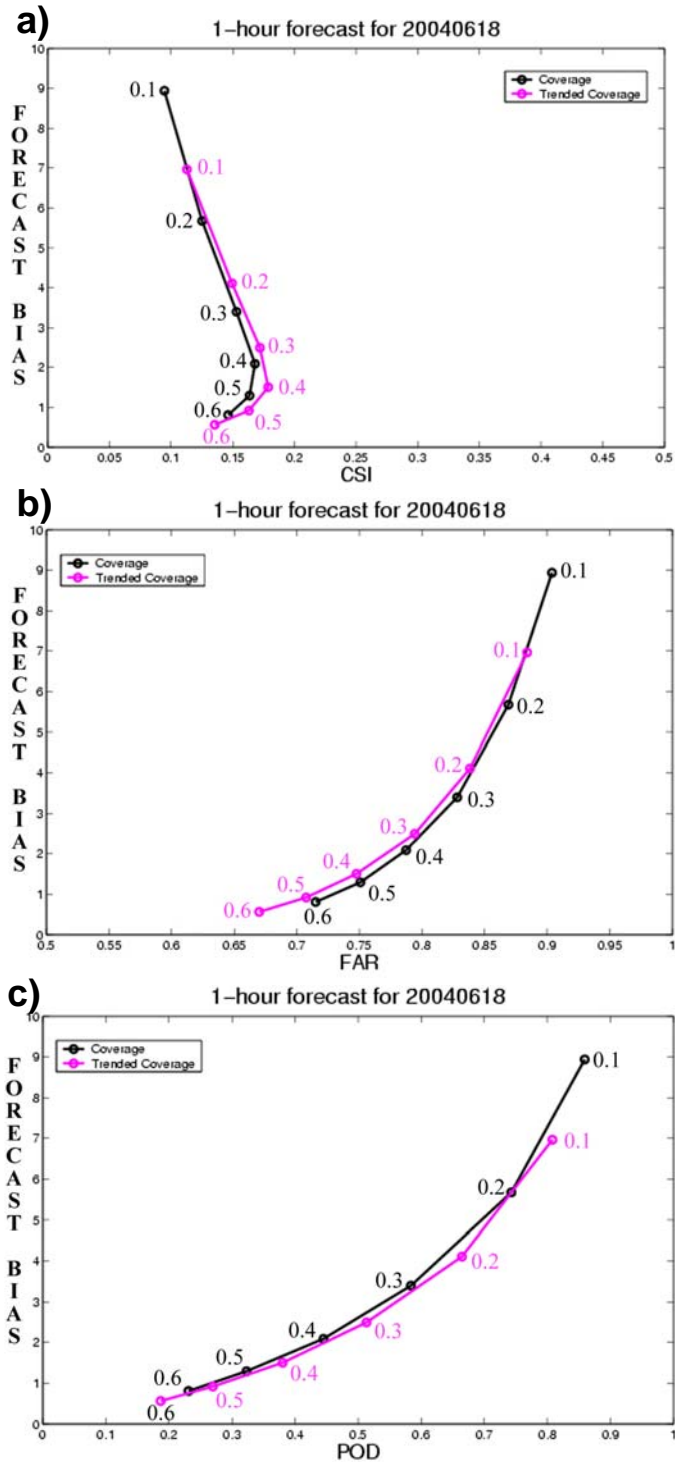


Figure 4 Figures 4a, 4b and 4c show the forecast bias (ratio between forecast area to observed area) versus the critical success index (or threat score), false alarm rate, and probability of detection, respectively. Validation statistics for trended (magenta lines) and non-trended (black lines) forecasts are shown. The probability levels are indicated numerically for trended (magenta) and non-trended (black) forecasts.

Statistical verification of the areas shown in Figures 2 and 3 over a 4-hour period are plotted in Figure 4. The data represent the forecast bias (ratio of forecast area to

observed area) versus the critical success index, or threat score, (Figure 4a), false alarm rate (Figure 4b), and probability of detection (Figure 4c). Validation

statistics for trended (magenta lines) and non-trended (black lines) forecasts are shown. The probability levels are indicated numerically. The decrease in forecast area coverage and bias between the trended and non-trended forecast results is greatest at low probability levels. In general, there is a slight improvement in CSI and POD for the trended forecasts (the magenta trended forecast line falls to the right of the black non-trended line) and FAR (the trended forecast values fall to the left of the non-trended values).

4 SUMMARY

A methodology to perform large-scale trending of radar data is presented. In the case shown here, large-scale trending of a storm line is effective. The calculated trends are very sensitive to inaccuracies and changes in the motion vectors used. Therefore, additional work must be done to improve these vectors. We hope to improve the trending results by trying to correct small errors in the motion vectors by looking in the neighborhood of the apparent previous location of each grid point for a location with a better fit to the current data.

5 REFERENCES

- Boldi, R. A., M. M. Wolfson, R. J. Johnson Jr., K. E. Theriault, B. E. Forman, and C. A. Wilson, 2002: An automated, operational two hour convective weather forecast for the corridor integrated weather. 10th Conf. on Aviation, Range, and Aerospace Meteorology, Portland, OR, 13-16 May, Amer. Met. Soc., Boston, 116-199.
- Dixon, M., and G. Wiener, 1993: TITAN: Thunderstorm identification, tracking, analysis and nowcasting – a radar-based methodology. *J. Atmos. Oceanic Tech.*, **10**, 785-797.
- Megenhardt, D, C. Mueller, S. Trier, D. Ahijevych, and N. Rehak, 2004: NCWF-2 Probabilistic Nowcasts. 11th Conference on Aviation, Range and Aerospace Meteorology, Hyannis, MA.
- Tsonis, A. A., and G. L. Austin, 1981: An evaluation of extrapolation techniques for the short-term prediction of rain amounts. *Atmos.-Ocean*, **19**, 54-65.
- Wilson, J.W., N. A. Crook, C. K. Mueller, J. Sun and M. Dixon, 1998: Nowcasting Thunderstorms: A Status Report. *Bull. Amer. Meteor. Soc.*, **79**, 2079-2099.
- Wolfson, M.M., B.E. Forman, K.T. Calden, W.J. Dupree, R.J. Johnson Jr., R.A. Boldi, C.A. Wilson, P.E. Bieringer, E.B. Mann and J.P. Morgan, 2004: Tactical 0-2 Hour Convective Weather Forecasts for FAA. 11th Conference on Aviation, Range and Aerospace Meteorology, Hyannis, MA.